2D - Finite Element Model of a CIGS Module

G.J.M. Janssen, L.H. Slooff, and E.E. Bende

ECN Solar Energy, P.O.Box 1, NL-1755 ZG Petten, The Netherlands

***Abstract* — The performance of thin-film CIGS modules is often limited due to inhomogeneities in CIGS layers. A 2-dimensional Finite Element Model for CIGS modules is presented that predicts the impact of such inhomogeneities on the module performance. Results are presented of a module with a region of poor diode characteristics. It is concluded that according to this model the effects of poor diodes depend strongly on their location in the module and on their dispersion over the module surface. Due to its generic character the model can also be applied to other series connections of photovoltaic cells.**

***Index Terms* — modeling, simulation, finite element method, CIGS, photovoltaic module**

I. Introduction

A successful implementation of thin-film CIGS technology still requires a reduction of the gap in efficiency between laboratory-scale cells and modules [1,2]. The CIGS module efficiency is often limited by inhomogeneities that originate from the layer deposition steps in the manufacturing process. Such inhomogeneities may be translated into local variations of the diode saturation current, the contact resistance, the shunt resistance, the photogeneration current, or combinations thereof [3,4].

Experimental techniques such as electro- or photoluminescence or thermography can be used to identify poor or 'bad' areas in the module. The effect of these bad areas on the module performance cannot always be easily estimated using analytical models [5-8]. The distributed series resistance of the contact layers has to be taken into account, as well as the monolithic series connection of the cells in a module. The finite conductivity of the contact layers implies that an individual CIGS solar cell cannot be described by a set of parallel one-diode equivalent circuits operating at the same voltage [5]. Additionally, the monolithic contact over the full cell length makes that a simple series connection of the individual cells is also not always a valid approach. Moreover, due to the manufacturing process that involves deposition of layers over the whole module surface area, bad areas can extend over more than one cell [7,8].

A model that takes into account the 2D spatial distribution of properties of the 'bad' areas over the module surface, is required for an accurate performance prediction. This can be implemented by describing the module by a network of 1-diode equivalent circuits that are coupled through the conductive contact layers. Finite element methods (FEM) are a suitable tool to solve the 2-D partial differential equations that form the basis of such a model.

In this paper we present the model for a *n*-cell CIGS module. However, due to its generic character the model is not limited to CIGS but can be applied to other photovoltaic modules as well. The model can predict the performance at various operation conditions (illumination, temperature, imposed current or voltage). In addition to overall performance data of the module such as *I-V* characteristics and efficiency, the voltage and current distribution in each cell can be obtained as well as the heat dissipated in the active layer and in the connecting and contact layers. Results will be presented that were obtained for the case of bad areas being represented by a high dark saturation current density j_0. The importance of the spatial resolution of the bad areas will be illustrated by calculations for single cells as well as 4-cell modules.

II. Model

A CIGS module consists of *n* cells with width *w* and length *L*. In the present model each cell is considered to consist of an active layer and two contact layers. The active layer can be a CIGS absorber layer with a CdS buffer layer. The properties of this layer are described by a local diode saturation current density j_0, an ideality factor *A*, and a shunt resistance R_{shunt}. The contact layers are the Transparent Conductive Oxide layer, e.g. ZnO:Al, and a Mo layer. These layers are characterized by their conductivity σ and thickness *t*. An additional contact resistance between the active layer and a contact layer may be included. The monolithic series connection is implemented by connecting the ZnO:Al layer of one cell to the Mo layer of the adjacent cell, over the whole length of the cell. Although in this model the thickness, length and conductivity of the connecting layer can be specified at will, we apply here the usual configuration of the monolithic

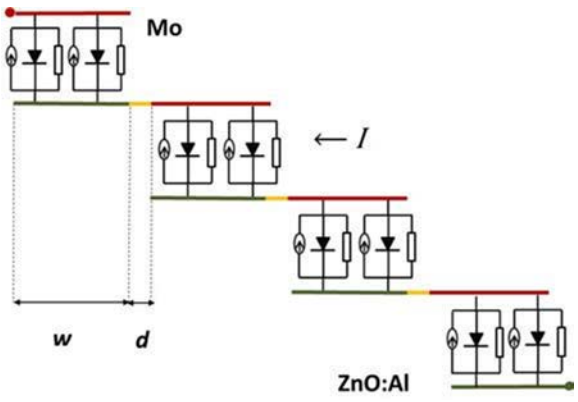

Fig. 1 Schematic showing the equivalent circuit representation of four cells connected in series.

TABLE 1
PARAMETERS USED IN THE CALCULATIONS

Parameter	Value	Parameter	Value
L	10 cm	j_L	34 mAcm^{-2}
w	0.5 cm	A	1.245
d	2 µm	j_0 good	50.6 fAcm^{-2}
s	160 µm	j_0 bad	5.06 µAcm^{-2}
t ZnO:Al	1 µm	R_{shunt}	1 kOhmcm^2
t Mo	1 µm	σ ZnO:Al	450 Scm^{-1}
T	298.15 K	σ Mo	$3\cdot10^4$ Scm^{-1}

CIGS interconnect [6]. This means that the conductivity is that of ZnO:Al. The length of the connect is equal to the thickness of the active layer d. The thickness of the connecting layer is s, *i.e.* the width of the scribe made between the active layers. The model is completed by defining a photogeneration current density j_L.

A schematic drawing showing the model layout for a 4-cell module is shown in Fig. 1. In this figure the red lines represent Mo layers, the green lines ZnO:Al layers, and the yellow lines the interconnects. Although only two equivalent circuits are drawn per cell, each cell is in fact represented by a large number of 1-diode circuits, both in the direction of the plane of the paper (cell width) and in the direction perpendicular to the paper (cell length). The module is contacted at the Mo layer of the cell on top of the structure and at the ZnO:Al layer at the bottom. It is assumed that the contacting is over the full cell length.

As mentioned above, all physical parameters included can be made dependent upon the (x, y) position in the module, i.e. they have a spatial distribution. In the present study only the dark saturation current density was made position dependent. Moreover, no contact resistance was assumed between the active layer and the contact layers. The model solves the distribution of the potential u in the n+1 conductive layers shown in the Fig. 1. Depending on whether the position in the layer corresponds to Mo, to ZnO:Al, or to the interconnect the equivalent circuits act as sources or sinks of current, or they do not contribute at all (interconnect region). For n cells this approach leads to a set of n+1 coupled 2-dimensional non-linear Poisson equations for the local potential u.

The boundary conditions are those of zero current, i.e. $\nabla u \cdot \mathbf{n} = 0$ at all boundaries except where the module is contacted. At these boundaries u=0 respectively $u=V_{module}$ is imposed. The equations are solved using a Finite Element Method, with a spatial resolution of about 4080 elements per cell. The values for physical parameters used in the calculations are listed in Table I.

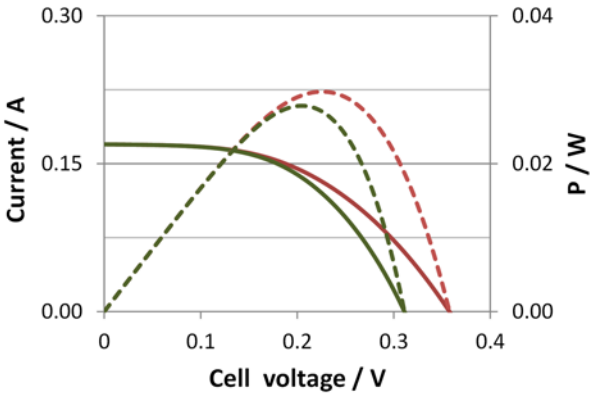

Fig. 2 *I-V* and *P-V* curve of a cell with 40% bad area uniformly distributed (green lines) and as a continuous, isolated area (red lines).

III. RESULTS

A. Single cell

With the parameters listed in Table 1, a single cell of 5 cm^2 without any bad zones has a V_{oc} of 650 mV. Neglecting the series resistance R_s that results from the finite conductivity of the contact layer, at the maximum power point (MPP) the power delivered by this cell is 88 mW. With the finite conductivity values the maximum power is in the order of 78 mW (see Table 2). This reduction is a combined effect of a locally increased potential difference across the active layer and dissipation of power in the contact layers (order 9 mW).

In a single cell a 'bad zone' was defined which comprised about 40% of the cell surface area. The values chosen for the dark saturation current density j_0 in the good and bad parts of the cell correspond to V_{oc} values of 650 mV and 282 mV, respectively. This large difference was chosen here to

TABLE 2
CHARACTERISTIC VALUES OF SINGLE CELLS

	V_{oc} V	I_{mp} A	V_{mp} V	P_{mp} mW	FF
Ideal, no R_s	0.650	0.158	0.556	88.0	0.80
Ideal with R_s	0.650	0.155	0.500	77.7	0.70
40% bad area, no R_s	0.311	0.149	0.242	36.1	0.68
40% distributed bad area with R_s	0.311	0.139	0.200	27.8	0.53
40% localized bad area with R_s *	0.352	0.129	0.230	29.7	0.49

*rectangular area as indicated in Fig. 3

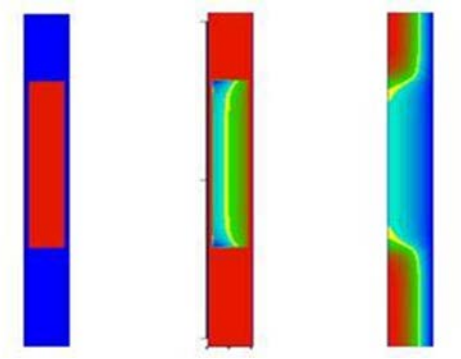

Fig. 3 From left to right: the distribution of the dark saturation current density j_0, of the generated current density at MPP, and of the cell voltage at MPP in a single cell with a bad area. The values increase from blue to red.

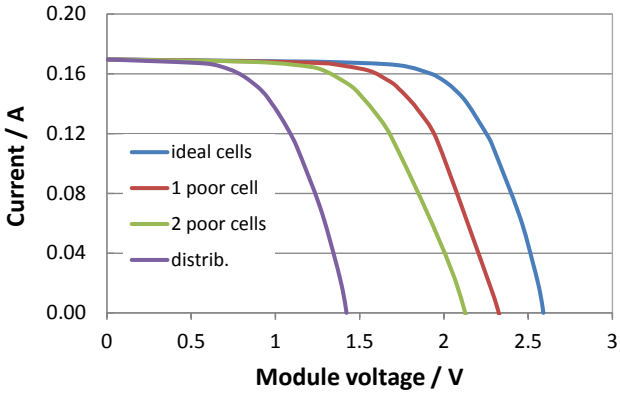

Fig. 4 *I-V* curves of a 4-cell module with all ideal cells and with 10% bad area localized in 1 or 2 cells, or uniformly distributed over the full module surface area.

highlight the effect of bad areas, but experimental data show that such variations can indeed be encountered in CIGS modules [8]. The area averaged value of j_0 results in 2.02 μAcm^{-2} with a corresponding V_{oc} of 311 mV. Table 2 shows the characteristic values that are obtained with such an averaged j_0 when the series resistance of the contact layer is ignored. Inclusion of the series resistances of the contact layers as specified in Table 1 results in a reduction of the maximum power from 36.1 mW to 27.8 mW and the fill factor *FF* from 0.68 to 0.53.

However, when a 2D FEM calculation is carried out that takes into account that the bad zone is a continuous, isolated part of the cell rather than distributed over the cell area, the maximum power and the V_{oc} increase from respectively 27.8 mW to 29.7 mW and 311 mV to 352 mV, as is also shown in Fig. 2. The *FF* and the current I_{mp} at the MPP on the other hand become lower (Table 2). This is a direct result of the shielding of the bad area that can take place due to finite conductivity of particularly the ZnO:Al layer. When the series resistance is put to zero, a calculation with spatial information on the bad zone geometry gives the same results as a calculation with an area averaged j_0. The reason for this is that without series resistance the potential difference over the active layer is the same all over the cell. This means that the position of a 1-diode circuit with a bad j_0 is not relevant, only the total fraction of such circuits.

The shielding effect is further demonstrated in Fig. 3. The generated current density distribution reflects very well the area of bad diode characteristics. Fig 3 shows that the cell voltage distribution is also not homogeneous. The local cell voltage outside the bad zone is higher than inside the bad zone. At open circuit conditions this is still the case. This reduces the current that needs to be dissipated in the bad zone and enhances the V_{oc} (Fig. 2, Table 2). The difference in local cell voltage corresponds to the potential distribution in the ZnO:Al layer. As a result of the inhomogeneity the current flow is squeezed to the areas outside the bad zone, which has a negative impact on the *FF*.

B. Four-cell module

The *I-V* curve of a four-cell module with ideal cells can be straightforwardly calculated from the single cell curve by multiplying all voltages by four. This results in the data of Table 3. The series resistance of the monolithic interconnect is in the order of μ-ohms and is therefore negligible.

TABLE 3
CHARACTERISTIC VALUES OF MODULES

	V_{oc} V	I_{mp} A	V_{mp} V	P_{mp} mW	*FF*
4 ideal cells	2.600	0.155	2.000	310.7	0.70
Bad area localized in one cell*	2.325	0.153	1.706	260.8	0.66
Bad area localized in 2 adjacent cells*	2.121	0.149	1.477	220.2	0.61
Uniform distribution of bad area*	1.421	0.145	0.948	137.4	0.57

*The total fraction of bad area was 10% of the total module active area.

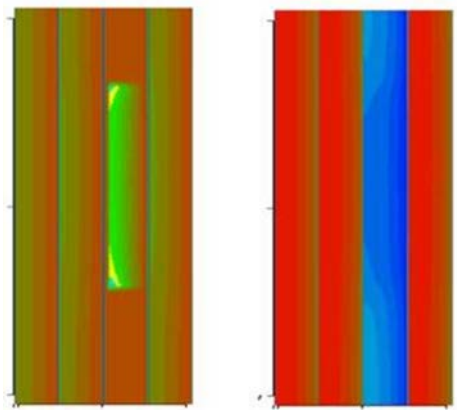

Fig. 5 On the left the distribution of the generated current density at MPP, and on the right of the cell voltage at MPP over the surface of the 4-cell module with the third cell from the left containing a bad zone as indicated in Figure 3. Blue: the lower value. Red: the higher value.

A module with 10% bad area can be constructed by embedding a poor cell as described above in a module with three ideal cells. The resulting *I-V* characteristics show a reduced V_{oc} and maximum power as well as fill factor (Fig. 4 and Table 3). The V_{oc} value is 2325 mV, i.e. the sum of three times the V_{oc} of the ideal cell and of the V_{oc} of the poor cell including shielding as given in Table 2. The maximum power point of the module is at a current that is quite close to the value of the ideal cells which means that the ideal cells are still delivering almost their maximum power and the penalty of the mismatch in I_{mp} is in the poor cell which now delivers only 28 mW. Fig. 5 shows that if the effect of the bad area is confined to one cell, the generated current density and cell potential of the other cells seem undisturbed.

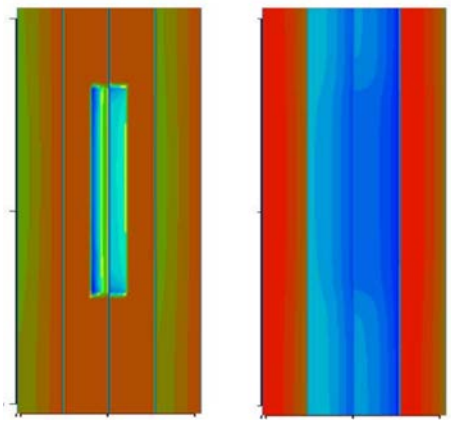

Fig. 6 On the left the distribution of the generated current density at MPP, and on the right of the cell voltage at MPP over the surface of the 4-cell module. With respect to Figure 5 the bad zone was now moved to the left, divided equally over the second and third cell. Red: the higher value. Blue: the lower value.

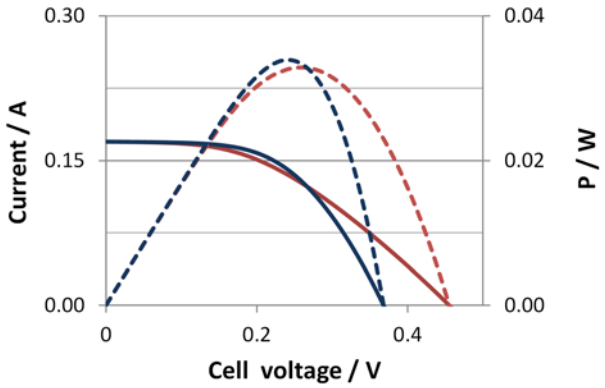

Fig. 7 *I-V* and *P-V* curves of a cell with 20% bad area located in the right half of cell (blue lines) and in the left half of the cell (red lines). These configuration correspond to the configuration of the bad areas in the second and third cell of the 4-cell module of Fig. 6

Fig. 4 shows that a shift of the poor zone towards a position where it is divided equally over two cells results in a much poorer module performance. The data in Table 3 confirm this. The V_{oc} shifts downwards by another 200 mV, and the MPP is now at 1477 mV producing only 220 mW. Figure 6 shows that at the point of maximum power two of the four cells have a significant area of reduced cell voltage. The average cell voltage in the ideal cells is 507 mV, in the second cell from the left 230 mV and in the third cell 198 mV.

The behavior of the two poor cells can be understood by considering two single cells, one with a bad zone at the right side, such as in the second cell of the module, and one with a bad zone the left side, such as in the third cell of the module. The right side is where the potential in the ZnO:Al layer is highest, and the cell voltage lowest. The left side is an area close to the zero current boundary of the ZnO:Al (see Fig. 1). The *I-V* and power curves of the two cells with 20% bad area in Fig. 7 show the effect the position of the bad area has on the cell performance. When the bad zone is at the left hand side, variation over the defect area of cell potential leads to an increased V_{oc} at the expense of a much lower *FF*.

At open circuit a series connection of cells implies that each cell is at open circuit conditions. Although both cells with 20% bad area have a V_{oc} higher than a cell with 40% bad area, the total impact on the module V_{oc} is larger.

The I_{mp} of the poor cells is also much reduced, and more in the third cell with the bad zone at the left side than in the second cell. At the maximum power point of the module the system tries to stay as close as possible to the optimum conditions of the cells contributing most, which are the ideal cells. The module I_{mp} is therefore close to the I_{mp} of the ideal

cells. This means that the weakest cell, i.e. the third cell with the lowest I_{mp}, operates furthest from its MPP and hence takes most of the penalty.

Still it can be inferred from Fig. 4 and Table 3 that this distribution of bad zones leads to a much higher performance of the module than when the bad zones are dispersed over the module surface area.

IV. Discussion

The analysis presented here shows that the impact of inhomogeneities depends strongly on their location in the module. A very important role must be attributed to the distributed series resistance of the contact layers. As the single cell studies showed, the distributed series resistance allows for shielding of a bad area in a cell. As a result localized bad area zones are less detrimental for the performance than finely dispersed bad areas.

When a bad area extends over more than one cell, the shielding effect is reduced. Due to the inactive connecting zone, the bad area behaves more like a distributed bad area. The fraction of the total module power loss incurred by each cell increases with the total of current in the ZnO:Al layer in the region of the bad area.

These results also underline the difficulties that may arise with the interpretation of effective parameters extracted by fitting equations for an equivalent circuit based on a limited set of diodes to the experimental data, as already pointed out by Malm and Edoff [7].

The method presented here is quite generic for CIGS or thin film solar modules. The type of inhomogeneity is not limited to variations in the dark saturation current but can also include variations in photogeneration current, shunts as well as variation in the effective conductivity of the contact layers. Furthermore, the method can be extended with a more sophisticated treatment of the monolithic contact, inclusion of a grid on the ZnO:Al surface and contact resistances between the active layers and the Mo-contact layer.

V. Conclusions

A 2-dimensional Finite Element Model for CIGS modules was developed that predicts the impact of cell inhomogeneities on the module performance. The model consists of a 2D network of parallel 1-diode circuits that are coupled by conductive layers.

As an example, the case of a module containing an area with poor diode characteristics was presented. It was shown that the location of such an area strongly affects its impact on the module performance.

It was pointed out that the model can deal with other types of inhomogeneities as well. Moreover, due to the generic way problem is treated, it can also be adapted for other types of series connections of photovoltaic cells.

Acknowledgement

Part of this work was undertaken in the context of the project “SOPHIA – Solar Photovoltaic European Research Infrastructure”. SOPHIA is a project supported by the European Commission in the 7th Framework Programme (GA n°262533). For further information about SOPHIA see: www.sophia-ri.eu.

References

[1] B. von Roederen, "National Solar Technology Roadmap CIGS PV", NREL/MP-520-41737 (2007).

[2] I. Repins, S. Glynn, J. Duenow, T. J. Couts, W. K. Metzger, and M. A. Contrera, "Required materials properties for high-efficiency CIGS modules", Proc.SPIE 7409, 74090M (2009).

[3] P. Mack, T. Ott, F. Schwäble, F. Runai, and T. Walter, "2D-Network simulation and modelling of CIGS modules", 25th PVSEC, Valencia (2010).

[4] T. Ott, F. R. Runai, F. Schwäble, and T. Walter, "2D network simulation and luminescence characterization of Cu(In,Ga)Se2 thin film modules", Prog.Photovolt: Res.Appl. DOI 10.1002/pip (2012).

[5] P. O. Grabitz, U. Rau, and J. H. Werner, "Modeling of spatially inhomogeneous solar cells by a multi-diode approach", Phys.Stat.Sol.(a) 202, 2920-2927 (2005).

[6] K. Brecl, M. Topic, and F. Smole, "A detailed study of monolithic contacts and electrical losses in a large-area thin-film module", Prog.Photovolt: Res.Appl. 13, 297-310 (2005).

[7] U. Malm and M. Edoff, "Influence from front contact sheet resistance on extracted diode parameters in CIGS solar cells", Prog.Photovolt: Res.Appl. 16, 113-121 (2008).

[8] U. Malm and M. Edoff, "Simulating material inhomogeneities and defects in CIGS thin-film solar cells", Prog.Photovolt: Res.Appl. 17, 306-314 (2009).